ELSEVIER J. Non-Newtonian Fluid Mech., 52 (1994) 387–405

Journal of Non-Newtonian Fluid Mechanics

Rheological characterization of the time and strain dependence for polyisobutylene solutions

R.F. Liang [1], M.R. Mackley *

Department of Chemical Engineering, University of Cambridge, Pembroke Street, Cambridge CB2 3RA, UK

(Received March 4, 1994)

Abstract

The rheological response of polyisobutylene (PIB) solutions in Decalin and a related standard fluid S1 has been characterized in dynamic oscillatory flow, step strain, step-shear rate and steady shear using a Rheometrics RDSII rheometer. The time dependence represented as a discrete spectrum of relaxation times and the strain dependence characterized as an exponential damping function have been presented as a function of PIB concentration. The relaxation spectrum was calculated from the dynamic storage modulus and loss modulus. The damping function was determined from the non-linear relaxation modulus in a step-strain experiment. The Wagner integral viscoelastic model incorporated with the relaxation and the damping function has been used to predict the stress growth and the steady-shear behaviour, which were compared with the experimental data. A novel extensional rheotester was also used in this study to measure the stretching response of polymer solutions. The data gave a near single relaxation time for each solution, and this single relaxation time obtained from uniaxial extension was correlated to the relaxation spectrum obtained in simple shear.

Keywords: Relaxation spectrum; Damping function; Filament stretching; Wagner integral viscoelastic model; Polyisobutylene solutions

1. Introduction

There is an increasing awareness that polymer melts in particular and a number of other rheological fluids in general can be characterized by considering a separable

* Corresponding author.

[1] Permanent address: Institute of Chemistry, Academia Sinica, Beijing 100080, China.

SSDI 0377-0257(94)01248-G

time dependence and a non-linear strain response. This approach originates from work by Wagner [1] and Laun [2], who showed that polyethylene melts could be characterized in this way. It is now possible to obtain commercial software where the time dependence in terms of a relaxation modulus of a material can be obtained, for example, from linear viscoelasticity measured [3–7]. In addition, the non-linear response often described in terms of a damping function can now be readily obtained from step-strain data using controlled-strain mechanical spectrometers [2,8,9].

Polyisobutylene, in the form of both pure melts and solutions, has been extensively studied, for example, in the field of elongational flow [10,11], second normal stress difference measurements [12–14], extensional viscosity measurements [15–19] and entry flow investigations [20–22]. As far as polyisobutylene solution is concerned, a detailed rheological study of two types of solution with different solvents has been reported by Quinzani et al. [23]. Rheological behaviour in steady-, oscillatory-, and transient-shear flows were measured and modelled with three differential constitutive equations (the Oldroyd-B model, the Giesekus model and the Bird–DeAguiar model) with four relaxation modes. A recent measurement of the extensional viscosity of polyisobutylene solutions has also been carried out by Sridhar and co-workers [17,18] using a filament stretching technique. Hudson and Jones [19] have given an overview on the rheology of the A1' fluid of polyisobutylene in decalin both in shear and extension. The integral constitutive equation of the K-BKZ type, proposed by Papanastasiou et al. [8], has been used to simulate numerically the entry flow of PIB solutions, and the results have been compared with experimental data [21,22]

In this paper, we extend the rheological characterization of PIB solutions in simple shear, and show that the approach of separable memory function and non-linear response can be successfully applied to a range of these fluids. The small-strain time-dependent relaxation spectrum and the non-linear response are both functions of the concentration. In addition, we show that an extensional measurement of the rheological response of the material surprisingly yields a near single relaxation time which can be correlated to an average relaxation time from the measured relaxation spectrum.

2. Choice of constitutive equation

A generalized, multiple Maxwell, linear viscoelastic model written in terms of the past strain deformation $\gamma(t, t')$ and the shear stress $\tau(t)$ is given by

$$\tau(t) = -\int_{-\infty}^{t} \sum_i \frac{g_i}{\lambda_i} e^{-(t-t')/\lambda_i} \gamma(t, t')\, dt', \tag{1}$$

where (g_i, λ_i) are discrete spectra of modulus and relaxation time, respectively, for the material. In order to describe non-linear effects, it is necessary to introduce a strain-dependent damping function into the equation. Different forms of damping function have been proposed [1,2,8,9,24]. In this work, an exponential damping

function, proposed by Wagner [1], is chosen because of its effectiveness and simplicity. Wagner's constitutive equation of the K-BKZ type in simple shear is then generalized as

$$\tau(t) = -\int_{-\infty}^{t} \sum_i \frac{g_i}{\lambda_i} e^{-(t-t')/\lambda_i} e^{-k|\gamma(t,t')|} \gamma(t, t')\, dt', \tag{2}$$

where k is the damping function coefficient.

The above constitutive equation is factorized in terms of the time and strain dependence of the polymer. The present work will check the validity of this equation in describing the rheological responses of PIB solutions. In order to apply eqn. (2), we obtain relaxation spectra (g_i, λ_i) from the oscillatory dynamic storage modulus and loss modulus by means of Rheometrics software. We determine the damping function coefficient from linear and non-linear step-strain experimental results. These material parameters are then combined into the equation to predict the transient-stress growth and the steady-shear behaviour. The self consistency can be identified from a comparison between the predicted and measured data in steady shear as well as in oscillatory shear and step strain.

Rheometric predictions of material functions from eqn. (2) are established in terms of the following deformations.

(1) Oscillatory response:

$$G'(\omega) = \sum_i \frac{g_i \omega^2 \lambda_i^2}{1 + \omega^2 \lambda_i^2}, \tag{3}$$

$$G''(\omega) = \sum_i \frac{g_i \omega \lambda_i}{1 + \omega^2 \lambda_i^2}, \tag{4}$$

$$\eta^*(\omega) = \sum_i \frac{g_i \lambda_i}{(1 + \omega^2 \lambda_i^2)^{1/2}}, \tag{5}$$

where $G'(\omega)$ is the storage modulus, $G''(\omega)$ is the loss modulus, ω is the oscillatory frequency, and $\eta^*(\omega)$ is a complex viscosity defined $(G'(\omega)^2 + G''(\omega)^2)^{1/2}/\omega$.

(2) Step strain:

$$G(\gamma_0, t) = \sum_i g_i e^{-t/\lambda_i}, \tag{6}$$

$$G(\gamma, t)/G(\gamma_0, t) = e^{-k|\gamma|}, \tag{7}$$

where $G(\gamma_0, t)$ is linear relaxation modulus at small strain γ_0 and $G(\gamma, t)$ is the non-linear relaxation modulus at large strain γ.

(3) Stress growth:

$$\tau(t, \dot\gamma) = \sum_i \frac{g_i \lambda_i \dot\gamma}{(1 + k\lambda_i \dot\gamma)^2} \{1 - e^{-(k\dot\gamma + 1/\lambda_i)t}[1 - k\dot\gamma t(1 + k\dot\gamma\lambda_i)]\}, \tag{8}$$

where $\dot\gamma$ is the step shear rate applied to the sample.

(4) Steady shear:

$$\eta_a(\dot{\gamma}) = \sum_i \frac{g_i \lambda_i}{(1 + k\lambda_i \dot{\gamma})^2}, \tag{9}$$

$$N_1(\dot{\gamma}) = 2\dot{\gamma}^2 \sum_i \frac{g_i \lambda_i^2}{(1 + k\lambda_i \dot{\gamma})^3}, \tag{10}$$

where $\eta_a(\dot{\gamma})$ is the apparent viscosity, $\dot{\gamma}$ is the shear rate, and $N_1(\dot{\gamma})$ is the first normal stress difference.

3. Materials and experimental

High molecular weight polyisobutylene (Vistanex) was supplied by Exxon Chemical Ltd., with an average molecular mass of $0.7-3.5 \times 10^6$ kg/kmol and a solid density of 920 kg/m^3. The solvent used was decahydronaphthalene (Decalin) with density 896 kg/m^3, viscosity 2.41 mPa s at 25°C and boiling point 190°C. The polybutene oil (PBO, HYVIS 10) was supplied by BP Chemicals for the preparation of the standard test fluid S1, with a density of 894 kg/m^3 and a viscosity of 31.3 Pa s. Polyisobutylene solutions were prepared by dispersing small readily soluble PIB pieces in Decalin, first without heating while stirring on a magnetic stirrer hotplate at 750 r.p.m., until all the PIB had been added, then increasing the temperature to 50°C and stirring for 8 h, and cooling to room temperature while still stirring at 500 r.p.m. for 3 or 4 days. The composition and concentration for PIB solutions are summarized in Table 1. The standard test fluid S1 was a 2.5% PIB in a mixed solvent of 47.5% Decalin and 50.0% PBO.

Rheological measurements were mainly carried out on a strain-controlled Rheometrics RDSII rheometer with ϕ50 mm cone/plate (ϕ25 mm cone/plate for sample A100 and S1) at 25°C. Material functions, as given in eqns. (3)–(10) for oscillatory, step-strain, step-share rate and steady shear were obtained and employed. The dynamic oscillatory and steady-shear experiments were also made on a stress-controlled Rheometrics DSR rheometer for comparison. It was confirmed that for polymer solutions, the rheological properties measured on the DSR were the same

Table 1
Polyisobutylene solutions tested

Sample	% (wt) PIB	Solvent
A20	1	Decalin
A40	2	Decalin
A60	3	Decalin
A80	4	Decalin
A100	5	Decalin
S1	2.5	47.5 Decalin/50.0% PBO

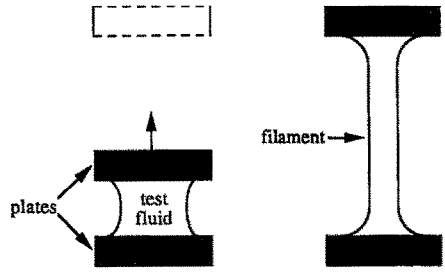

Fig. 1. Formation of a filament on the extensional rheotester.

as those measured on the RDSII, although the data from the DSR are limited to the relatively low deformation-rate range owing to the torque constraints of the instrument.

Experiments were also carried out using an extensional rheotester developed by Brazilevsky et al. [25]. The device consists of deforming and stretching the test fluid axially, and then following the subsequent diameter change of a thread line formed between the separated and subsequently fixed plates. The formation of a filament is schematically shown in Fig. 1. The stretching flow in the rheotester after the initial deformation is driven only by surface tension forces. Data are obtained on the time dependence of the thread diameter at a room temperature of 22°C. They are able to give the ratio of viscosity to surface tension for a Newtonian viscous fluid or a near single relaxation time for Maxwell viscoelastic fluids.

4. Rheometric characterization and prediction

Oscillatory shear flow

In order to obtain meaningful oscillatory shear data, it is necessary to carry out experiments within the linear strain range. The strain range for linear viscoelasticity is usually determined through a dynamic strain sweep at a fixed frequency. Figure 2 is the result of a dynamic strain sweep for all PIB solutions measured at a frequency of 20 rad/s. The complex viscosity was plotted against strain. As seen from Fig. 2, for all solutions, the complex viscosity remains independent of the strain up to 100%. This unusually wide linear strain range was also shown in the plots of storage and loss moduli against strain. In order to obtain noise-free stress data, a strain of 50% was used for all the subsequent linear viscoelasticity measurements, i.e. dynamic frequency sweeps.

Linear viscoelasticity measurements were made at 50% strain and in the frequency range of 10^{-1}–10^{2} rad/s to characterize the time dependence. A typical frequency sweep result for sample A100 is presented in Fig. 3. Complex viscosity, storage modulus and loss modulus are plotted as a function of frequency. Figure 3 shows that, as expected for polymer solutions, both the viscous modulus and the

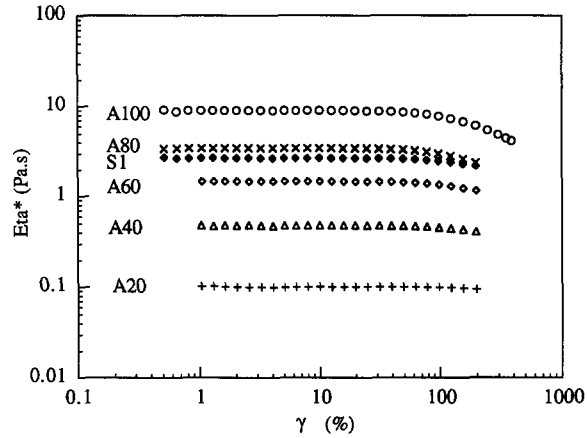

Fig. 2. Dynamic strain sweeps for all samples at a frequency of 20 rad/s.

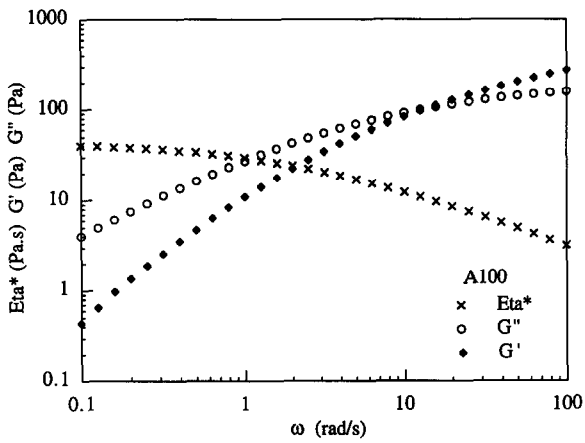

Fig. 3. Linear viscoelastic response for sample A100 at strain 50%.

elastic modulus increase with the oscillatory frequency. The viscous modulus dominates the response of the low-frequency range while the elastic modulus dominates the response of the high-frequency range. There is a crossover point at a moderate frequency where $\tan \delta = G''/G' = 1$.

The discrete relaxation spectrum can be conveniently calculated from dynamic $G'(\omega)$ and $G''(\omega)$ data using Rheometrics software. There are three methods available for this purpose: least square, regularization, and non-linear. At present, only the non-linear method can avoid negative values of the relaxation modulus (g_i) because there is a positive constraint for this numerical procedure [3,7]. For this reason, only the non-linear method was used in the present work. Eleven time constants (λ_i) were chosen spaced logarithmically and equally over a time scale of

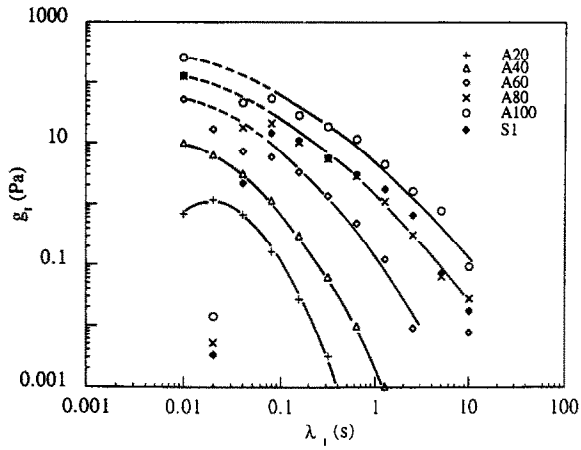

Fig. 4. Discrete relaxation spectrum (g_i, λ_i) with 11 time constants for all samples.

10^{-2} to 10 s in order that a good fit could be obtained between the measured and the predicted $G'(\omega)$ and $G''(\omega)$. The relaxation spectrum (g_i, λ_i) obtained for sample A100 is given in Fig. 4 where g_i was plotted against λ_i.

Similarly, from the dynamic oscillatory data of other samples we can also calculate (g_i, λ_i) data for each sample. The distribution of relaxation times for other PIB solutions studied is also plotted in Fig. 4. The results show that the values of the relaxation moduli generally decrease monotonically with increasing time constant for the range examined. The relaxation spectra increase both in weighting and range as the PIB concentration increases; this implies that as the PIB concentration increases, the viscoelasticity increases and relaxation processes of longer time scale become significant. The relaxation spectrum of the standard fluid S1 is nearly the same as that of sample A80. The lines plotted in Fig. 4 represent the approximate envelope of behaviour. For reasons that are not clear to us, the moduli of three solutions at $\lambda = 0.02$ s appeared to be lower than anticipated from the other data.

We can combine the relaxation spectrum (g_i, λ_i) data with eqns. (3) and (4) to check self consistency between the measured $G'(\omega)$ and $G''(\omega)$, and the predicted $G'(\omega)$ and $G''(\omega)$. The comparison is presented in Fig. 5(a) for the viscous modulus and in Fig. 5(b) for the elastic modulus for all PIB solutions. From Fig. 5, several points can be drawn: first, as the PIB concentration increases, both viscosity and elasticity increase significantly; secondly, there exists an excellent agreement between the experiment and prediction in the linear viscoelasticity range; thirdly, the S1 fluid shows almost the same viscoelastic response as sample A80.

Step strain

The damping function, as a non-linear measure, can be determined from step-strain experiments. A step-strain test applies a strain within the linear or non-linear

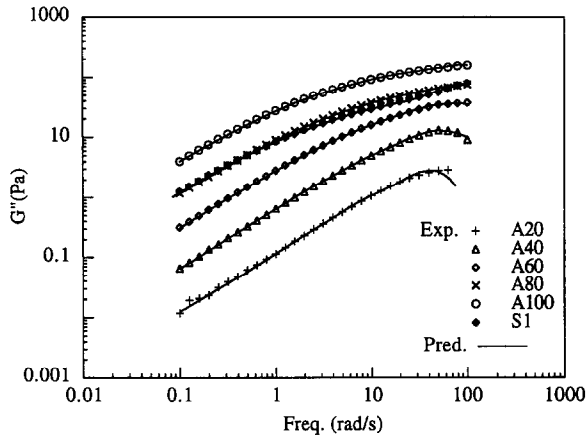

(a)

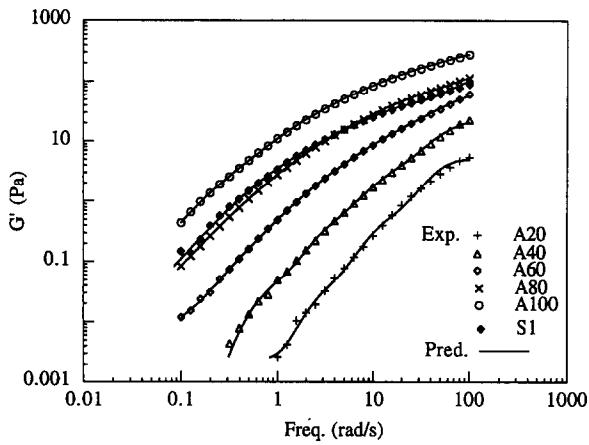

(b)

Fig. 5. Measured (symbols) and predicted (solid lines) dynamic moduli as functions of frequency for all samples at strain 50%. (a) $G''(\omega)$, (b) $G'(\omega)$.

strain range to the sample, and measures the stress or the modulus of decay with time. Figure 6 is a step-strain result for sample A100. The relaxation modulus, $G(t) = \tau(t)/\gamma$, is plotted as a function of time for the different applied step strains. It is found that the relaxation modulus decreases monotonically with time at a given strain. A non-linear effect is observed after a strain of 100%. As the step strain increases further, the relaxation modulus decreases with the same time dependence, but with the curve shifted vertically downward. This fact shows the factorable nature of the relaxation process, i.e. that the time dependence of the relaxation is independent of strain. Below 0.1 s on the time scale the relaxation modulus data is not separable and we believe this is due to a finite rise time effect (rise time is the time required for the instrument to response), which is a limitation of the rheometer.

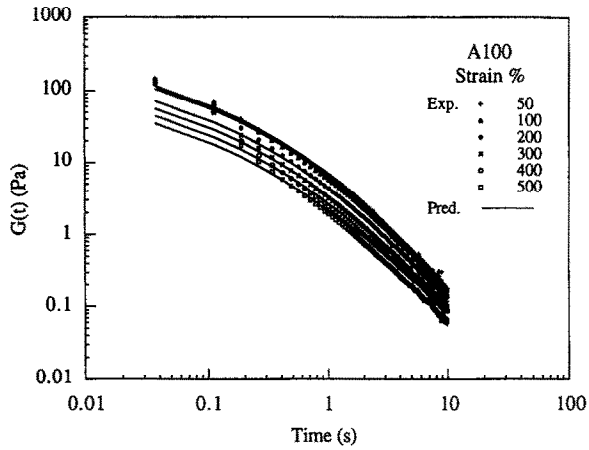

Fig. 6. Measured (symbols) and predicted (solid lines) relaxation moduli in step strain as functions of time for sample A100 at different strains.

From eqn. (7), the shear damping function coefficient k can be determined from the data of Fig. 6 and was found to be 0.24 for sample A100. From the step-strain experiment results of other samples, we can also calculate the damping function coefficient for each sample. The change of damping function with PIB concentration is shown in Fig. 7. It is found that the damping function coefficient increases non-linearly with PIB concentration, which suggests that it may plateau to a constant value at high concentrations.

It should be mentioned that the k value of the S1 fluid also fits the curve in Fig. 7. The damping function coefficient is equal to 0.14 for the S1 fluid. Thus, the S1 fluid has a smaller k value than that of sample A80 ($k = 0.21$), although their linear viscoelastic responses and relaxation spectrum are similar, as shown in Figs. 5 and 4, respectively. This fact suggests to us that non-inear rheological response mainly

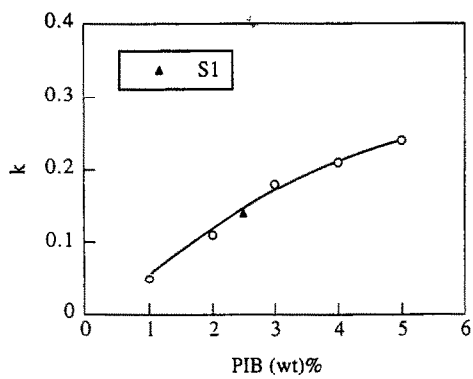

Fig. 7. Damping function as a function of PIB concentration.

results from the contribution of the high molecular weight polyisobutylene chain interaction. The solvent viscosity does not influence non-linearity since the S1 fluid is made up of 2.5% (wt) PIB dissolved in the mixture solvent with high viscosity (see Table 1). However, the high solvent viscosity indeed enhances the linear viscoelasticity.

The self consistency between the measured and the predicted relaxation moduli is checked. For sample A100, the predicted relaxation modulus is also plotted in Fig. 6 for different strains and compared with the experimental data. Excellent agreement is found for all samples.

Stress growth

An experiment to study the transient response of the material to a suddenly applied deformation is the step-shear rate test, which applies a constant shear rate to the sample and measures the growth stress with time. Figure 8 shows the results obtained from a step-shear rate experiment for the S1 fluid. A normalized stress (defined as the shear stress divided by the equilibrium stress value) is plotted against time. As seen from Fig. 8, the stress overshoot strength depends strongly on the shear rate applied. At a shear rate of 1 s^{-1}, the shear stress increases gradually with time to a steady equilibrium value and no stress overshoot occurs, implying that the material is able to follow the deformation. When the shear rate is 5 s^{-1}, the shear stress first increases to a maximum value and then decreases gradually with time to an equilibrium steady value, and a weak stress overshoot peak develops. This means that the material can no longer follow the start-up flow deformation, i.e. the response time scale of the material is longer than 0.2 s. At a shear rate of 50 s^{-1}, the material shows very marked stress overshoot behaviour. When a high shear rate is suddenly applied to the sample, the polymer chains are instantly stretched along the

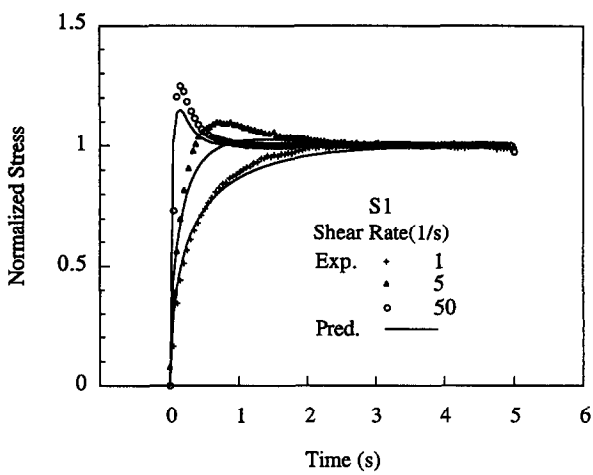

Fig. 8. Measured (symbols) and predicted (solid lines) normalized stress growth curves for the S1 fluid at three different shear rates.

shear direction. The stretched polymer chains then gradually relax to an equilibrium steady state. Therefore, stress overshoot occurs.

The stress growth response, both in shear and extension, is often used to test a constitutive equation. The predicted curve for three different shear rates from the model using eqn. (8) are plotted in Fig. 8. The stress overshoot peak is successfully predicted, for example, in the case of shear rate $50\,s^{-1}$, although the stress overshoot strength is underpredicted. Therefore, we can conclude that the model appears to predict the stress growth behaviour with reasonable accuracy.

Steady shear

Both the linear viscoelastic relaxation spectrum and the non-linear damping function can be used to predict the non-linear steady-shear behaviour. The apparent viscosity is predicted using eqn. (9). Figure 9 shows the comparison of the apparent viscosity between experiment and prediction for all PIB solutions. The apparent viscosity is plotted as a function of shear rate. As seen from Fig. 9, the solutions of low PIB concentration display very weak shear thinning behaviour. As the PIB concentration increases, the non-linear shear thinning behaviour becomes much stronger, corresponding to an increase in the magnitude of the damping function coefficient. The zero shear viscosity, i.e. the plateau value of apparent viscosity in the range of low shear rate, also increases significantly with concentration. It is found that, on a semi-logarithmic plot, the zero-shear viscosity increases linearly with the PIB concentration, except that the S1 fluid has the same zero-shear viscosity as A80, as seen in Fig. 9. In addition, it can be seen that, as expected from the discussion on step strain, sample A80 shows stronger shear thinning behaviour than the S1 fluid in spite of having the same zero shear viscosity.

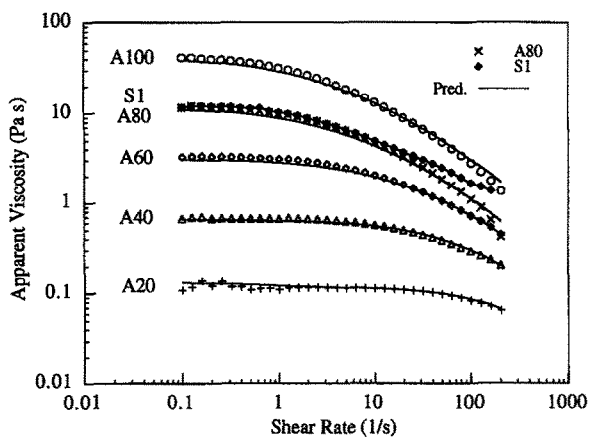

Fig. 9. Measured (symbols) and predicted (solid lines) apparent viscosities as functions of shear rate for all samples.

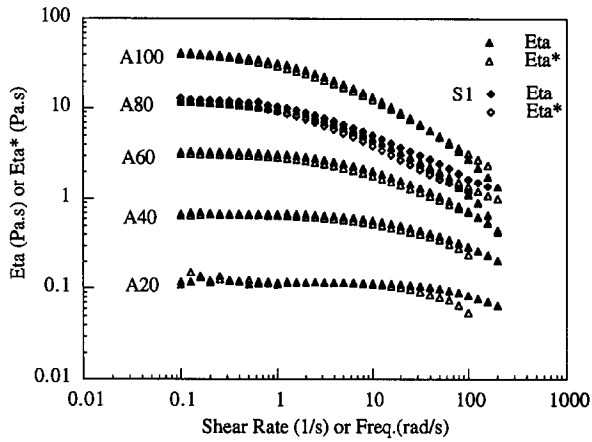

Fig. 10. Cox–Merz rule — comparison between the apparent viscosity and the complex viscosity for all samples.

Figure 9 also shows that the predicted apparent viscosity agrees very well with the measured apparent viscosity for each sample. This fact indicates the validity of describing the polymer solutions in terms of the Wagner constitutive equation used in this paper.

The complex viscosity is compared with the apparent viscosity as shown in Fig. 10 for the studied PIB solutions. Figure 10 shows that the Cox–Merz rule [26] is generally obeyed, although from eqns. (5) and (9) there is no reason to suppose that the oscillatory complex viscosity has to be equal to the steady-shear apparent viscosity when the frequency equals the shear rate. At high shear rates there is in fact a divergence in behaviour. For example, in the case of the S1 fluid, the complex viscosity and the apparent viscosity diverge at high rates, where they are both correctly predicted by the model but do not follow the Cox–Merz rule.

As a measure of elasticity of the material, the first normal stress difference (N_1) can also be measured in steady shear. The measured first normal stress difference data for the S1 fluid are plotted as a function of shear rate in Fig. 11. N_1 is found to increase nearly with the square of the shear rate in the range of the shear rate used. It is also observed that the ratio of N_1/τ^2 is almost constant, in agreement with the literature [19], and insensitive to the PIB concentration. The predicted N_1 data from the model based on eqn. (10) are represented by the solid line in Fig. 11. Reasonable agreement is found between the experiment and the prediction.

5. Extensional rheotester

The extensional rheotester is a device that has been developed by Bazilevsky et al. [25] at the Moscow Institute for Problems in Mechanics, Russian Academy of Sciences. It involves placing a drop of high-viscosity fluid between two discs and

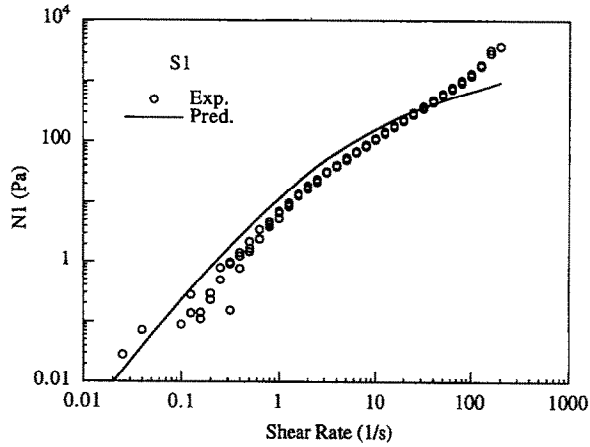

Fig. 11. Measured (circles) and predicted (solid line) first normal stress difference as a function of shear rate for the S1 fluid.

rapidly displacing the plates to a set displacement using a spring mechanism. The fluid is stretched between the plates to form a near-uniform thickness thread. This thread then thins under the combined action of surface tension and rheological forces. The thinning of the thread is followed optically and a filament diameter as a function of time is obtained.

Newtonian fluids

The thinning behaviour of a filament, driven by surface tension, is influenced by the fluid rheology. First of all, simple modelling of a Newtonian fluid subjected to the deformation of the rheotester can be described as follows.

Assume an incompressible cylindrical thread which is subjected to a surface tension. From a force balance, the total stress σ_{zz} in the axial direction and σ_{rr} in the radial direction are given by

$$\sigma_{zz} = -p_0 + 2\eta\dot{\gamma}_{zz} = 0, \tag{11}$$

$$\sigma_{zz} = -p_0 + 2\eta\dot{\gamma}_{rr} = -2\alpha/D, \tag{12}$$

where p_0 is the atmospheric pressure, η is the viscosity, α is the surface tension, D is the filament diameter, $\dot{\gamma}_{zz}$ is the strain rate along the axial direction z, and $\dot{\gamma}_{rr}$ is the strain rate along the radial direction r.

For uniform uniaxial extensional flow of an incompressible fluid with a strain rate $\dot{\epsilon}$, conservation of mass requires that the diameter of the filament decreases by

$$\dot{D} = -\tfrac{1}{2}\dot{\epsilon}D. \tag{13}$$

Define $\dot{\gamma}_{zz} = \dot{\epsilon}$, then $\dot{\gamma}_{rr} = -\dot{\epsilon}/2$.

Eliminating the pressure term from eqns. (11) and (12) yields the elongational stress

$$\sigma_E = \sigma_{zz} - \sigma_{rr} = 3\eta\dot{\epsilon} = 2\alpha/D. \tag{14}$$

From eqn. (14) we obtain the strain rate for a Newtonian fluid:

$$\dot{\epsilon} = 2\alpha/3\eta D. \tag{15}$$

Equation (15) shows that the strain rate will increase as the filament diameter decreases. Also, from eqn. (14), we obtain the extensional viscosity, η_E, defined as the elongational stress divided by the strain rate:

$$\eta_E = \sigma_E/\dot{\epsilon} = 3\eta. \tag{16}$$

As we know, the extensional viscosity of a Newtonian fluid is equal to three times the shear viscosity, independent of the strain rate.

Combining eqns. (13) and (15), and then integrating, yields the diameter of a Newtonian fluid thread as a function of time:

$$D(t) = D_0 - \alpha t/3\eta, \tag{17}$$

where D_0 is the initial diameter. Hence, for a Newtonian fluid, this simple model predicts that the diameter of the filament will decrease linearly with time.

In order to test the device, a high-viscosity Newtonian fluid, polydimethylsiloxane (PDMS), was used. The change in diameter with time is plotted in Fig. 12. The diameter decreases nearly with time. From the slope and eqn. (17), the ratio of viscosity to surface tension, $\eta/\alpha = 1.18 \times 10^4$ s/m, can be obtained. From the

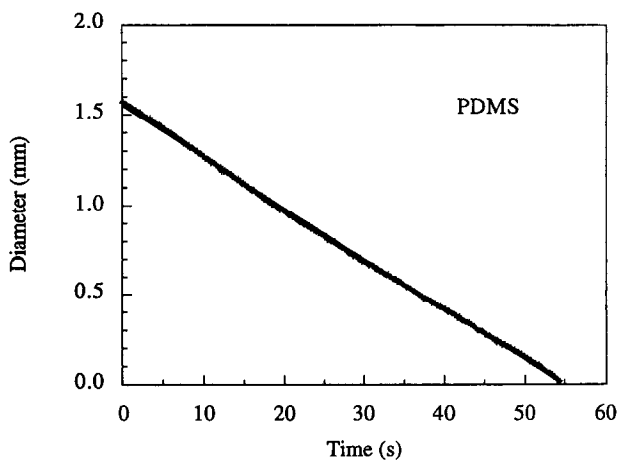

Fig. 12. Filament diameter as a function of time for PDMS. The parameters in eqn. (17) are fitted to the data: $D_0 = 1.55$ mm, $\eta/\alpha = 1.18 \times 10^4$ s m^{-1}

separate viscosity measurement, $\eta = 115$ Pa s, which yields $\alpha = 9.74 \times 10^{-3}$ N/m for the fluid PDMS.

Viscoelastic fluids

The A-series polymer solution and S1 fluid were tested using the extensional rheotester and the diameter decay of each sample is shown in Figs. 13(a) and 13(b). To a first approximation, the curves fit a single exponential relaxation time defined as the rheotester relaxation time λ_R [25], where

$$D(t) = D_0 \exp(-t/3\lambda_R). \tag{18}$$

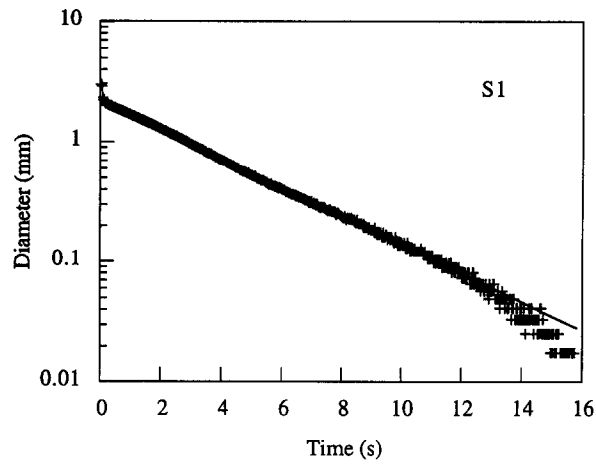

(a)

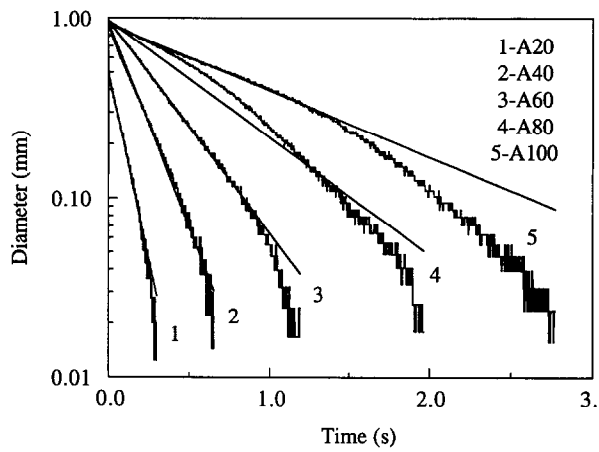

(b)

Fig. 13. Filament diameters as functions of time for the PIB solutions: (a) S1 fluid, (b) other PIB solutions. The solid lines are data-fit lines from eqn. (18). The parameters of the S1 fluid are, for example, $D_0 = 2.44$ mm, $\lambda_R = 1.12$ s.

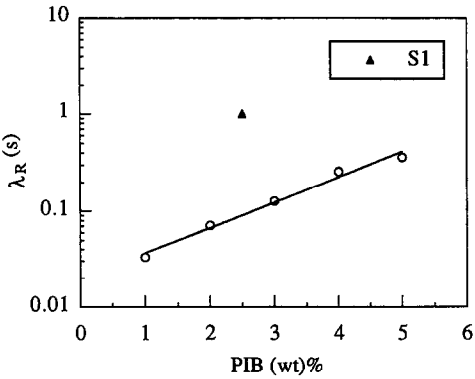

Fig. 14. Rheotester relaxation time as a function of PIB concentration.

This rheotester relaxation time is plotted in Fig. 14 as a function of PIB concentration and, with the exception of the S1 solution, the A- series polymer solutions show a monotonic increase in λ_R with increasing concentration.

We were initially very surprised that the rheotester should give a single relaxation time for viscoelastic fluids that give multiple relaxation times in simple shear. Modelling the flow using Maxwell-type equations and/or the Wagner integral form does not appear to give the experimentally observed response. However, it is possible to provide an alternative simple rheological model that gives a consistent prediction when compared with the extensional results.

Following Hinch [27], we assume that when a viscoelastic fluid is used, the tensile stress in the fluid is balanced by the elastic properties, and the stresses due to viscosity and surface tension are equal, then

$$\sigma_E = 3\eta\dot{\epsilon}_d = 2\alpha/D, \tag{19}$$

where $\dot{\epsilon}_d$ is the linear viscous 'dashpot' strain rate and η is the shear viscosity of the dashpot. In addition, we equate the rate of change of stress associated with elasticity to the corresponding surface tension stress rate of change, giving

$$\dot{\sigma}_E = g\dot{\epsilon}_s = -2\alpha\dot{D}/D^2, \tag{20}$$

where $\dot{\epsilon}_s$ is the strain rate for the linear elastic 'spring' and g is the elastic spring modulus.

We also assume that the strain rate associated with the elastic deformation is the same as that associated with the viscous component:

$$\dot{\epsilon}_d = \dot{\epsilon}_s. \tag{21}$$

Combining eqns. (19) and (20) with eqn. (21) yields

$$\dot{D}/D = -g/3\eta. \tag{22}$$

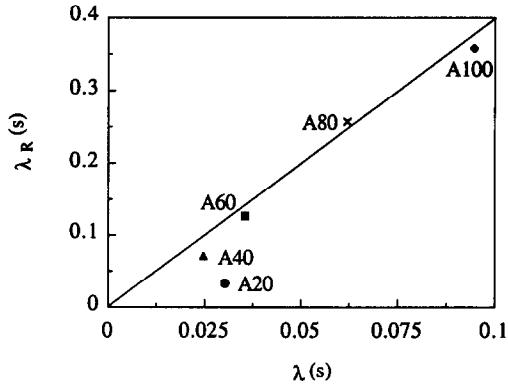

Fig. 15. Correlation of the rheotester relaxation time with the mean relaxation time.

Integration of this equation yields

$$D(t) = D_0 \exp\left(-\frac{g}{3\eta}t\right), \tag{23}$$

which is of the required form. Defining $\lambda_R = \eta/g$ yields eqn. (18). Using the mass balance equation, eqn. (13), yields the overall strain rate for the viscoelastic fluid:

$$\dot{\epsilon} = 2g/3\eta. \tag{24}$$

Therefore, the strain rate of a viscoelastic fluid is a constant.

If we further assume a discrete spectrum of linear viscoelastic elements and assume

$$\sigma_E = \sum \sigma_i = \sum 3\eta_i \dot{\epsilon}_{di} = \dot{\epsilon}_d \sum 3\eta_i, \tag{25}$$

$$\dot{\sigma}_E = \sum \dot{\sigma}_i = \sum g_i \dot{\epsilon}_{si} = \dot{\epsilon}_s \sum g_i, \tag{26}$$

then

$$D(t) = D_0 \exp(-t/3\bar{\lambda}), \tag{27}$$

where

$$\bar{\lambda} = \sum 3\eta_i \Big/ \sum g_i = \sum 3g_i\lambda_i \Big/ \sum g_i. \tag{28}$$

In Fig. 15, we plot the rheotester relaxation time in terms of $\bar{\lambda}$, the mean relaxation time obtained from the simple shear data. There is a near linear relationship between the rheotester relaxation time and the mean relaxation time $\bar{\lambda}$ measured from the G' and G'' data, however, the rheotester relaxation time is nearly a factor of three greater than $\bar{\lambda}$. The correlation with the S1 fluid is less satisfactory, for which $\lambda_R = 1.12$ s and $\bar{\lambda} = 0.073$ s.

6. Conclusions

The present work has rheologically characterized the time and strain dependence in simple shear of some PIB solutions, and indicated the factorable nature of the shows an excellent self consistency between small-strain oscillatory and step-strain data. Rheological responses in step-shear rate and steady shear, as well as in oscillatory and step strain, can be modelled with reasonable accuracy using Wagner's constitutive equation combined with a spectrum of relaxation times and an exponential damping function. It is found that the relaxation spectrum increases both in weighting and range with increasing polyisobutylene concentration. The damping function coefficient, as a measure of non-linear effect, also increases with PIB concentration.

The measurement of the stretching behaviour of these polymer solutions using an extensional rheotester gives a near single relaxation time for each sample. This relaxation time for uniaxial extension is also found to increase with PIB concentration and correlates to a mean relaxation time determined from the relaxation spectrum in simple shear. The fact that the rheotester gives a single exponential relaxation time where simple-shear measurements give a broad spectrum is an initially surprising result. A modelling of the extensional flow behaviour is given to explain the single exponential behaviour. It would appear that the extensional behaviour of these solutions follows a different rheological behaviour to simple shear, and it is speculated that the free rotation nature of the extensional flow modifies the rheology when compared with simple shearing rheology which contains a rotational component of flow.

The S1 fluid is composed of 2.5% PIB in a mixture solvent of 47.5% Decalin and 50% PBO, while sample A80 is made up of 4% PIB in Decalin. In simple shear it is found that the S1 fluid possesses nearly the same relaxation spectrum as sample A80, but a smaller damping function than sample A80. However, the response of the S1 fluid in uniaxial extension as measured by the rheotester is different from those of other PIB solutions and yields a much longer relaxation time. The presence of PBO appears to have a more significant effect on the extensional behaviour than on the simple-shear behaviour. The observation that the rheotester relaxation time is a factor of three larger than the simple shear relaxation time $\bar{\lambda}$, suggests that relaxation process measured by the rheotester originates from stretched polymer chains that can exhibit longer relaxation times than unstretched chains (see, for example, Hinch [28] and de Gennes [29]).

Acknowledgements

The authors would, in particular, like to thank Dr. John Hinch (DAMTP, University of Cambridge) for his assistance and interest in the rheotester work, and Professor Jim Ferguson of the University of Strathclyde for providing the S1 fluid and polyisobutylene melt. R.L. would also like to thank the Royal Society and the National Physical Laboratory for the support which made it possible for him to carry out the work reported in this paper.

References

1 M.H. Wagner, Rheol. Acta, 15 (1976) 136–142.
2 H.M. Laun, Rheol. Acta, 17 (1978) 1.
3 M. Baumgaertel and H.H. Winter, Rheol. Acta, 28 (1989) 511–519.
4 M. Baumgaertel and H.H. Winter, J. Non-Newtonian Fluid Mech., 44 (1992) 15–36.
5 J. Honerkamp and J. Weese, Macromolecules, 22 (1989) 4372.
6 V.M. Kamath and M.R. Mackley, J. Non-Newtonian Fluid Mech., 32 (1989) 119.
7 N. Orbey and J.M. Dealy, J. Rheol., 35 (1991) 1035–1049.
8 A.C. Papanastasiou, L.E. Scriven and C.W. Macosko, J. Rheol., 27 (1983) 387–410.
9 P. Soskey and H.H. Winter, J. Rheol., 28 (1984) 625.
10 A. Demarmels and J. Meissner, Colloid Polym. Sci., 264 (1986) 829–846.
11 M.H. Wagner and A. Demarmels, J. Rheol., 34 (1990) 943–958.
12 G.A. Alvarez, A.S. Lodge and H.J. Cantow, Rheol. Acta, 24 (1985) 368–376.
13 A.S. Lodge, T.S.R. Alhadithi and K. Walters, Rheol. Acta, 26 (1987) 516–521.
14 J.J. Magda, J. Lou, S.G. Baek and K.L. Devries, Polymer, 32 (1991) 2000–2009.
15 T. Sridhar, J. Non-Newtonian Fluid Mech., 35 (1990) 85.
16 D.M. Binding, D.M. Jones and K. Walters, J. Non-Newtonian Fluid Mech., 35 (1990) 121.
17 T. Sridhar, V. Tirtaatmadja, D.A. Nguyen and R.K. Gupta, J. Non-Newtonian Fluid Mech., 40 (1991) 271–280.
18 V. Tirtaatmadja and T. Sridhar, J. Rheol., 37 (1993) 1081–1102.
19 N.E. Hudson and T.E.R. Jones, J. Non-Newtonian Fluid Mech., 46 (1993) 69.
20 M.S. Chai and Y.L. Yeow, J. Non-Newtonian Fluid Mech., 35 (1990) 459.
21 H.J. Park and E. Mitsoulis, J. Non-Newtonian Fluid Mech., 42 (1992) 301–314.
22 E. Mitsoulis, J.Rheol., 37 (1993) 1029–1040.
23 L.M. Quinzani, G.H. Mckinley, R.A. Brown and R.C. Armstrong, J. Rheol., 34 (1990) 705–748.
24 H.C. Booij and J.H.M. Palmen, Rheol. Acta, 219 (1982) 376–387.
25 A.V. Bazilevsky, V.M. Entov and A.N. Rozhkov, in D.R. Oliver (Ed.) Proc. 3rd European Rheology Conference, Edinburgh, UK, Elsevier Science Publishers, London and New York, 1990, pp. 41–43.
26 W.P. Cox and E.H. Merz, J. Polym. Sci., 28 (1958) 619.
27 E.J. Hinch, private communication, 1994.
28 E.J. Hinch, Polymères et Lubrification, Colloques Internationaux du C.N.R.S., 233 (1974) 241–247.
29 P.G. de Gennes, J. Chem. Phys., 60 (1974) 5030–5042.